JOURNAL OF APPLIED ELECTROCHEMISTRY 22 (1992) 916–921

Further studies of a zinc–air cell employing a packed bed anode
Part II: Regeneration of zinc particles and electrolyte by fluidized bed electrodeposition

T. HUH*, G. SAVASKAN, J. W. EVANS

Materials Science Division, Lawrence Berkeley Laboratory/Department of Materials Science and Mineral Engineering, University of California, Berkeley, CA 94720, U.S.A.

Received 22 August 1991; accepted 20 January 1992

Fluidized bed zinc electrodeposition appears to be an efficient way of regenerating zinc particles and electrolyte from the discharge products of the cell described in Part I. Using a laboratory cell, various electrode materials were examined to determine their suitability for this electrodeposition. The effects of current density and zincate concentration on the performance of the cell were determined. The lowest d.c. electrical energy consumption achieved was 1.92 kWh kg^{-1} of zinc at 1000 A m^{-2} superficial current density. The corresponding figure at 2000 A m^{-2} was 2.08 kWh kg^{-1}. Combining these values with the results of Part I, the 'roundtrip' electrical energy efficiencies of a system employing the cell of Part I for discharge, and fluidized bed electrodeposition for recharge, are 50% and 46%, respectively.

1. Introduction and previous investigations

The fluidized bed electrode has been the subject of many investigations concerned with the electrodeposition of metals from aqueous solution. The electrode might offer advantages in terms of capital cost as a result of the high space-time yield achievable in such a cell and possibly in terms of reduced electrical energy consumption [1]. In the context of electrical energy storage, the high surface area and high mass transfer rate means an electrode wherein energy can be stored without excessive parasitic losses due to overvoltages.

Recently Evans and Savaskan invented the mechanically rechargeable zinc–air battery employing a particulate packed bed anode [2, 3] (see Part I). The concept behind the cell is mechanical recharging. Residual particles and electrolyte are removed from the battery near the end of discharge and replaced with fresh particles and electrolyte, which are electrochemically regenerated from cell discharge products in a local or regional facility. The generation of fresh zinc particles directly from strong alkaline solution would be a crucial step in the application of this zinc–air battery and would only be possible by using large electrochemical reactors such as a fluidized bed reactor. The investigation described in the present paper was intended as a test, on a laboratory scale, of whether such regeneration is practicable. Under SFUDS discharge as described in Part I, the discharge is halted when the voltage falls below a practical value, rather than when the voltage becomes zero. At the former point no precipitation has occurred and the electrolyte is clear. The processing of products removed from the cell is then simply one of redeposition of zinc onto the particles.

The cathodic behaviour of zinc electrode in alkaline solutions has been extensively studied for battery applications. These investigations may be divided basically into two categories. Those in one were focused on elucidating the fundamental electrochemical reduction reaction mechanism [4, 7, 9, 10] and obtaining quantitative information on the kinetics of this system [5, 6, 8]. Those in the other category dealt with the effects of operating conditions on the zinc deposit morphology during reduction reaction with the aim of improving the limited cycle life of zinc batteries [11–14].

It has been well established that tetrahydroxy zincate anion ($Zn(OH)_4^{2-}$) is a predominant zinc ionic species in alkaline solution and the reduction mechanism of zincate to metallic zinc consists of a complicated series of reactions [4–8]. It also appears that the three most important morphologies associated with zinc deposition from alkaline solutions are smooth, mossy and dendritic deposits, that dendrite growth occurs during diffusion limited conditions, and that the rate of growth rather than the rate of nucleation is the controlling factor in determining the morphology [11, 12, 14].

In fluidized bed electrodeposition, particles experience fluctuating overpotentials [15] and mechanical impact during particle–particle collision. Also, mass transfer rates should be high due to the small particles

* T. Huh (deceased) was with the Department of Metallurgical Engineering, Pusan National University, Pusan, Korea.

0021-891X/92

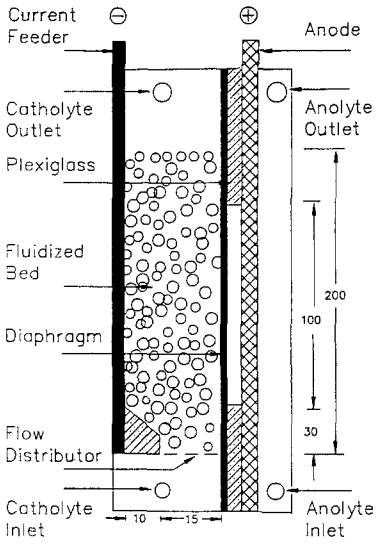

Fig. 1. Side view of laboratory scale cell with modified distributor for fluidized cathode. (All dimensions in millimetres, not scaled.)

and their motion [16]. Therefore zinc deposits on particles within the fluidized bed electrode should be smooth.

Since the fundamental mechanism of this reaction is not within the scope of the present study, the single step reaction [4–8],

$$Zn(OH)_4^{2-} + 2e^- \longrightarrow Zn + 4OH^-$$
$$E^0 = -1.25\,V/SHE \qquad (1)$$

is considered as the zinc reduction reaction at the cathode and the oxygen evolution reaction,

$$4OH^- \longrightarrow O_2 + 2H_2O + 4e^-$$
$$E^0 = 0.401\,V/SHE \qquad (2)$$

as the oxidation reaction at the anode. It has been reported that the only possible secondary reaction at a zinc cathode in pure potassium hydroxide solution would be hydrogen evolution [9, 10] which is as follows:

$$2H_2O + 2e^- \longrightarrow H_2 + 2OH^-$$
$$E^0 = -0.828\,V/SHE \qquad (3)$$

The present paper reports on the feasibility of the fluidized bed electrodeposition process as a recharging step for the mechanically rechargeable zinc–air battery. By using a laboratory scale fluidized bed electrode, the effects of superficial current density, current feeder materials, anode materials and diaphragms on the performance of zinc electrodeposition were investigated.

2. Experimental details and apparatus

Figure 1 depicts the 50 A cell, used in this investigation, which is similar to that used in the previous investigations of fluidized bed electrodeposition at Berkeley [15] except at the bottom of the bed.

Previously it was found that the performance of a fluidized bed electrode was dependent on various operating parameters, especially on bed expansion [19]. The bed expansion, which represents the degree of fluidization, affects the particle density throughout the bed and consequently the effective bed resistivity. Because the latter affects the electric current path through the bed, the electrochemical reaction rate distribution through the bed depends on the bed expansion. When bed expansion was kept around 25%, fluidized bed electrodeposition was free from any operating problems. However when bed expansion was less than 25%, there was a decrease in effective bed resistivity, causing an increase of the electrochemical reaction rates in the vicinity of the diaphragm. In this case, the usual result was metal deposition on the diaphragm, which is one of the operating problems of fluidized bed electrodeposition. Conversely, when bed expansion was kept much above 25%, metal was deposited on the current feeder. This was because high effective bed resistivity resulted in the preferential current path being through the electrolyte within the bed to the vicinity of the current feeder where electrochemical reaction would then take place.

In preliminary work it was found that there was a tendency for zinc deposition on the current feeder. To keep the effective resistivity of the bed near the current feeder low, and consequently to overcome the problem of zinc deposition on the current feeder, the flow distributor was redesigned so that the inflow of electrolyte was near the diaphragm, rather than uniformly across the bed. With this cell configuration, the particle movement in the bed became a recirculating motion, going upward rapidly near the diaphragm and falling down slowly near the current feeder. This circulating motion of particles enabled the electrode to be operated with the bed expansion as low as 18–20%. The effective resistivity of the bed near the current feeder was then low and that of the other side of the bed high to prevent zinc deposition at both sides of the bed.

The cell employed a cathode consisting of a fluidized bed of 500 μm copper particles which were coated with zinc in preliminary experiments. It is believed that in a practical zinc–air battery based on the cell in Part I, the zinc would be present as a coating on an inert substrate and the battery would be designed so that discharge is halted before all the zinc has been oxidized. This is the justification for using zinc-coated copper particles in the present investigations, although it is anticipated that better inert substrates than dense copper would be used in practice.

When expanded, the modified fluidized bed cathode measured approximately 25 mm × 70 mm × 200 mm high. Current feeders of graphite (4 mm thick); copper (1 mm) or lead (4 mm) were used. A platinized titanium mesh, a nickel mesh, DSA (a titanium mesh with a proprietary coating, which is catalytic for oxygen evolution, Eltech. Corp.) and NE-A-30 anode (a nickel mesh with a catalytic coating for oxygen evolution in strong alkaline solution, Electrolyser Corp.) were tested as an anode. The anode and cathode compartments were separated by a flexible porous plastic diaphragm

(either "Daramic", W. R. Grace Corp. or "Celgard", Hoechst Celanese Corp.), which has very low permeability to electrolyte and enables the use of different compositions of anolyte and catholyte. The diaphragm was supported by a 6 mm thick plexiglass sheet with a 50 mm × 100 mm opening ("window"), which served as the active area of the diaphragm. The bottom of the window was kept 30 mm above the distributor.

The catholytes used were prepared by dissolving zinc oxide (AR, Fisher Scientific) into 45% potassium hydroxide solution (AR, Fisher Scientific). The anolyte used was 25% potassium hydroxide solution, selected because it is more conductive than 45% potassium hydroxide solution.

The experimental procedure consisted of filling each reservoir. The pumps were turned on and the particles added to the cathode chamber. The catholyte flow rate was adjusted to bring the bed expansion to the desired level. The current to the cell (supplied by a Hewlett Packard 6261 B d.c. power supply operated in an amperostatic mode) was turned on and the electrolysis commenced. The current and the cell voltage were monitored on a strip chart recorder. The catholyte was sampled periodically and the samples were analysed for zinc by complexometric titration using EDTA. Titration was performed twice for each sample and the zinc concentrations were reproducible with much less than one percent of difference. The current efficiencies were calculated from zinc depletion of the catholyte for each time interval and averaged for an entire run. With this average and with the cell voltage, the electric energy consumption was calculated.

3. Experimental results and discussion

Electrical energy consumption was considered the main quantity of interest in determining the feasibility of the fluidized bed electrodeposition process as a recharging step for the zinc–air battery. Because electrical energy consumption is directly dependent on the current efficiency and cell voltage, most of the results were expressed in terms of these two variables.

Figure 2 shows the dependence of cell voltage on superficial current density (current per unit active area of the 50 mm × 100 mm window of the diaphragm). All results of Fig. 2 are for a fluidized bed electrode with graphite current feeder, Daramic diaphragm and nickel mesh anode. During long runs with Daramic diaphragms, as will be described in detail later, a gradual cell voltage increase was noticed after about an hour of electrolysis at 2000 A m^{-2}. Therefore all cell voltage data for polarization were gathered after approximately a half hour of electrolysis, when the cell voltage was stable. The top line in Fig. 2 is for the original fluidized bed (uniform distribution of flow across the bed), the second line is for the original fluidized bed with a lower active window area and the bottom line is for the fluidized bed electrode modified as shown in Fig. 1. The bed expansion of the modified fluidized bed electrode was 18–20%, and for the others was 25%. Figure 2 shows that cells with the same configuration exhibit identical voltage variation regardless of zinc concentration in the range shown. That is, the cell voltage was not affected by zinc concentration during the electrodeposition from alkaline solution unless the concentration dropped to a few grams per dm^3, whereupon hydrogen started to evolve. The figure also shows that the cell voltage can be reduced by modifying the fluidized bed. By moving the active window area of the diaphragm down towards the distributor by 20 mm, lower cell voltage can be achieved. However with this configuration, not unexpectedly, zinc was deposited on the diaphragm after 2 h at 2000 A m^{-2}. In a previous study [15], it was found that in a fluidized bed electrode the particle density is higher at the bottom of the bed. This means that the effective resistivity of the bottom part of the bed is lower than in the rest of the bed and the bottom of the bed would serve as a path for most of the current. Therefore in fluidized bed electrodeposition, it is normal to keep the current distribution uniform throughout the bed by maintaining a certain distance (usually 20–30 mm) between the window and distributor. In the case of the cell with a lowered window, much of the current passed through the bottom part of the bed with electrochemical reaction in the vicinity of the diaphragm, which resulted in zinc deposition on the diaphragm. With the modified electrode (Fig. 1), the cell voltage was 0.2 to 0.7 V less than in cells with the original electrode. It was found that the cell voltage of the fluidized bed electrode was lowered by decreasing bed expansion down to 18–20% without any operating difficulties.

Figure 3 shows the cell voltage against superficial

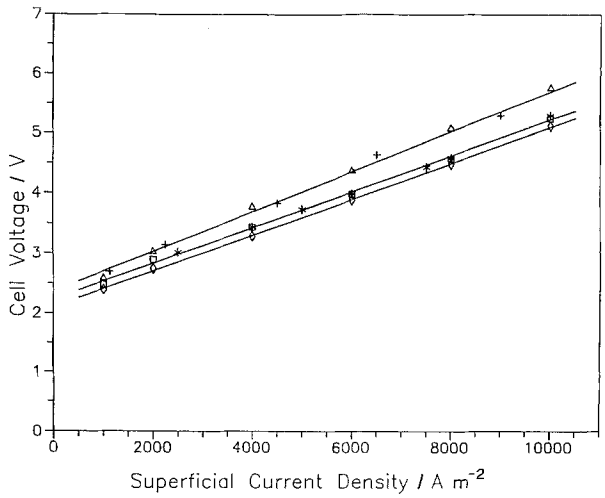

Fig. 2. Effect of cell configuration on cell voltage. (Current feeder: graphite; diaphragm: Daramic; anode: Ni mesh.)

	Zn conc. ($g\,dm^{-3}$)	*FBE*
(△)	45	original
(+)	30	original
(*)	20	window down
(□)	25	window down
(◇)	25	modified

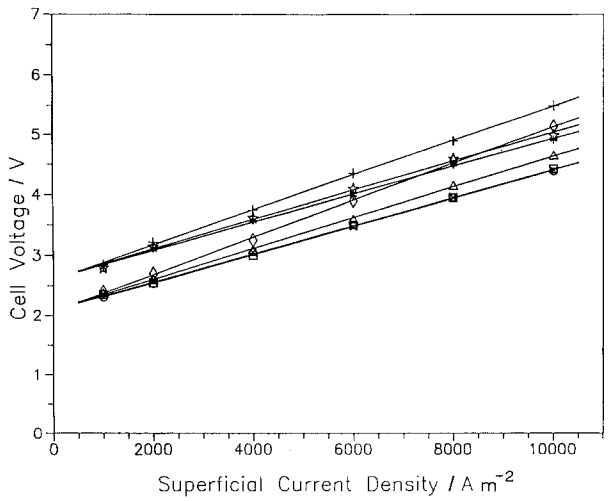

Fig. 3. Effect of electrode materials on cell voltage. (CCF: cathode current feeder and C, Cu, Pb for graphite, copper, lead respectively. Ni, Pt, DSA, NE-A-30 for nickel mesh, platinized titanium mesh, Dimensionally Stable Anode and NE-A-30 anode, respectively.)

	CCF	*Anode*	*Zn conc.* ($g\,dm^{-3}$)
(+)	C	Pt	26
(◇)	C	Ni	20
(☆)	Cu	Pt	19
(△)	C	DSA	26
(□)	Cu	DSA	20
(*)	Pb	Pt	17
(×)	Pb	DSA	21
(○)	Pb	NE-A-30	25

current density for the modified fluidized bed electrodes with various anodes and current feeders, which were separated by a Daramic diaphragm. From the cell voltage point of view, copper and lead current feeders showed almost similar behaviour. Cells with those current feeders and either DSA or NE-A-30 anodes showed the lowest numbers and graphite current feeder and platinized titanium mesh anode system showed the highest throughout the superficial current density range tested. The relative resistivities (measured by the four-probe method using a precision multimeter), of graphite, copper and lead current feeders were 1020, 1.55 and 18.2 $\mu\Omega$ cm respectively. Thus, despite being thicker, the graphite feeder can be expected to result in a much greater voltage drop than the other two, which are both sufficiently conductive to have little effect on cell voltage.

To determine the effects of anode materials on cell voltage, anode voltages were measured with respect to a Hg/HgO reference electrode. As mentioned before, the voltage of the cell with a Daramic diaphragm was not stable throughout the electrolysis. Results are shown in Fig. 4. All were measured at the superficial current density of 2000 A m^{-2}. The cells used each had a lead current feeder and a Daramic diaphragm, but a different anode, as noted. The top three lines are voltage variations of each cell and the bottom three are anode voltages against a Hg/HgO reference electrode, the capillary tip of which was placed at the centre of the active area on the diaphragm side of the anode. Even though the voltages of the Pt and NE-A-30

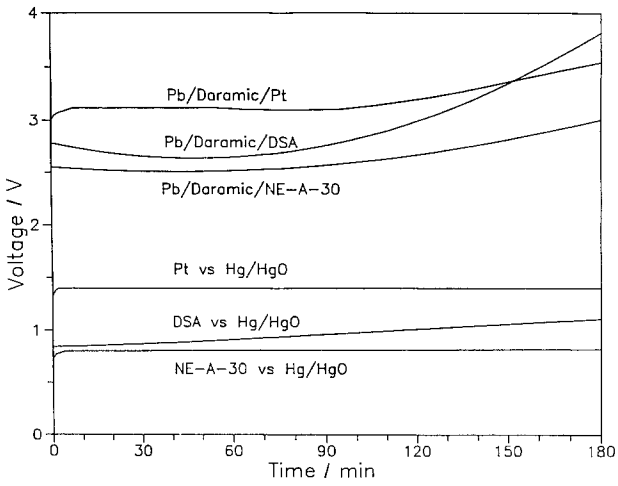

Fig. 4. Cell and anode voltage variations of cells with Daramic diaphragms during electrodeposition at 2000 A m^{-2} superficial current density. (Initial zinc concentrations of cells with Pt, DSA and NE-A-30 anodes were 27, 21 and 26 g dm^{-3}, respectively.)

anodes were stable, the voltages of cells with these anodes increased gradually in a similar way. The differences between cell voltages were the same as those between anode voltages. The voltage of the DSA exhibited instability during the electrolysis, which resulted in additional variation of cell voltage.

Daramic appears to shrink when exposed to strong alkaline electrolytes, and this may result in loss of porosity (and therefore conductivity), leading to the cell voltage increases seen in Fig. 4. This is confirmed in Fig. 5 where it is seen that cells with Celgard diaphragms show stable voltages which are also lower than those of cells with Daramic diaphragms. Polarization curves for the two types of diaphragms (after approximately 30 min of electrolysis) appear in Fig. 6, showing that the Celgard diaphragm appears superior over a broad current density range.

The other variable which directly affects the energy consumption is the current efficiency. Plots of current efficiencies of the cell with different current feeders are shown as a function of zinc concentration in Fig. 7.

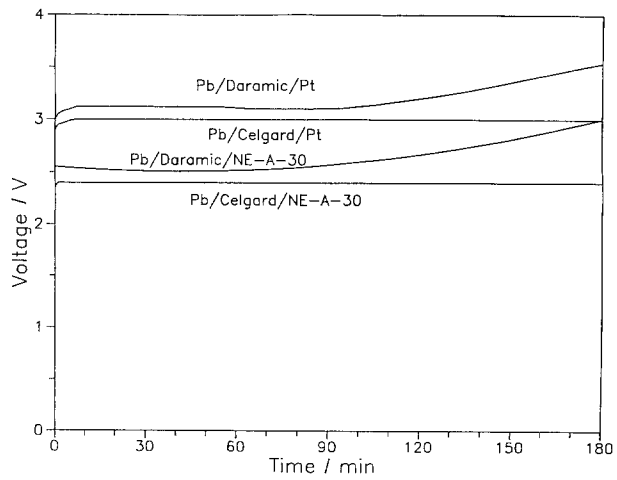

Fig. 5. Effect of diaphragm on cell voltage stability during electrodeposition at 2000 A m^{-2} of superficial current density. (Initial zinc concentrations of Pb/Daramic/Pt, Pb/Celgard/Pt, Pb/Daramic/NE-A-30 and Pb/Celgard/NE-A-30 were 27, 25, 26 and 25 g dm^{-3}, respectively.)

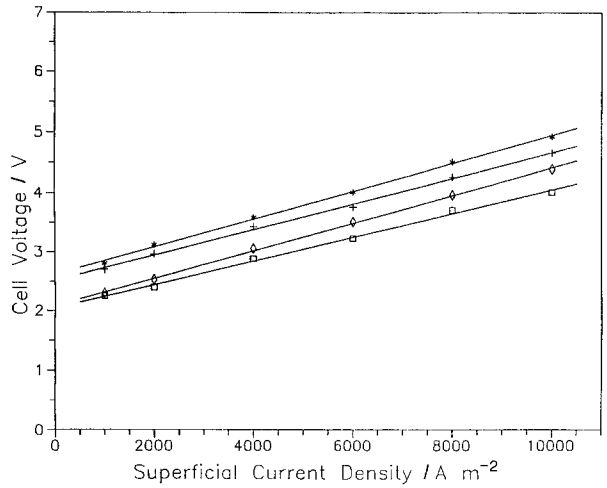

Fig. 6. Effect of diaphragm on polarizations of the cells with identical electrodes.

		Zn conc. (g dm^{-3})
(*)	Pb/Daramic/Pt	25
(+)	Pb/Celgard/Pt	24
(◇)	Pb/Daramic/NE-A-30	23
(□)	Pb/Celgard/NE-A-30	24

The superficial current density of all runs was kept at 2000 A m^{-2}. In this figure each data point represents an average current efficiency over a concentration range (covering 3 to 20 g dm^{-3} of zinc) centred about the concentration indicated by the data point. In all cases current efficiencies remained almost constant down to the zinc concentration of a few dm^3, which means zinc can be recovered with reasonably high current efficiency for a wide range of zinc concentration by fluidized bed electrolysis. Below that concentration, current inefficiency, which is caused by hydrogen evolution, became severe. Down to this concentration limit, the electrodes with graphite and lead current feeders showed approximately 94 to 95% current efficiency and that with copper showed 88%. The relatively low current efficiency of the electrode with

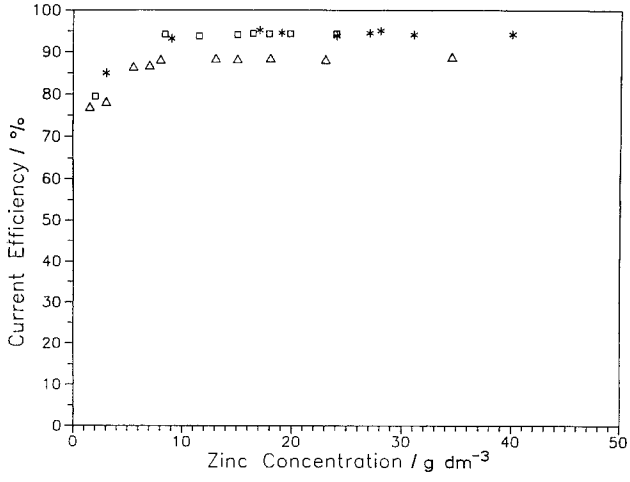

Fig. 7. Plots of current efficiency against zinc concentration for the fluidized bed cathode with different current feeders. (All are at 2000 A m^{-2} of superficial current density.) Current feeder: (*) graphite, (△) copper and (□) lead.

Table 1. Summary of the performance of fluidized bed electrodeposition of zinc from 45% KOH zincate solutions at 2000 A m^{-2} of superficial current density (except where indicated)

*Electrodes** CCF	Dia	Anode	*Cell volt†/ V*	*Zinc conc./ g dm^{-3}*	*CE‡/ %*	*Energy cons./ kWh kg^{-1} Zn*
C	DAR[1]	DSA	2.65	20.0–14.3	94.6	2.29
C	DAR	Ni	2.81	34.0–28.3	94.6	2.44
C	DAR	Pt	3.22	26.0–12.6	94.6	2.79
Cu	DAR	Pt	3.15	25.7–10.4	87.9	2.94
Pb	DAR	Pt	3.12	27.2–13.8	94.3	2.71
Cu	DAR	DSA	2.57	22.1–19.3	87.9	2.40
Pb	DAR	DSA	2.58	21.6–18.2	94.3	2.24
Pb	DAR	NEA[2]	2.53	25.5–14.1	94.3	2.20
Pb	Cel[3]	Pt	2.96	24.8–12.6	94.3	2.57
Pb	Cel	DSA	2.45	21.6–10.1	94.3	2.13
Pb	Cel	NEA	2.40	24.6–13.9	94.3	2.08
Pb	Cel	NEA	2.22[4]	16.4–11.3	94.8	1.92
Pb	Cel	NEA	2.88[5]	24.7–11.4	90.7	2.60

* Fluidized bed electrode, cathode current feeder, diaphragm, anode.
† Cell voltages for the cells with Daramic diaphragm were averaged during the electrolysis.
‡ Current efficiencies were averaged over a run.
1 Daramic.
2 NE-A-30 anode.
3 Celgard.
4 With 1000 A m^{-2} of superficial current density.
5 With 4000 A m^{-2} of superficial current density.

copper current feeder is considered partially due to low hydrogen overvoltage on a copper surface [17]. A similar conclusion results from the current efficiency variation during the initial stage of zinc deposition on fresh copper particles from 45% potassium hydroxide zincate solution; the average current efficiency during each hour of electrodeposition was increased from 52% for the first hour to 93% for the fourth hour with a graphite current feeder. It seems that increasing current efficiency results from metamorphosis of the actual electrochemical reaction front from a copper surface to a zinc surface. This also can be explained by a study [13] on the effects of copper substrate on zinc deposition. It was reported that copper substrates might encourage the growth of active hexagonal zinc deposits with many kink sites and edges, the surface area of which increased with thickness and this also resulted in an increase in the dissolution activity of the zinc deposit with increasing deposit thickness. Therefore it can be concluded that the existence of a copper surface which is electrochemically active in the cell would lower the current efficiency of zinc electrowinning from alkaline solution.

Table 1 summarizes the present study. The effects of electrode materials on the performance of the fluidized bed electrodeposition cell at a superficial current density of 2000 A m^{-2} are shown. For each different cell system, cell voltage, current efficiency and electrical energy consumption are presented. The current efficiencies for each current feeder material were averaged. As explained before, cells with lead and graphite current feeders behaved similarly from the current efficiency point of view, and those with copper and lead current feeders behaved similarly from the

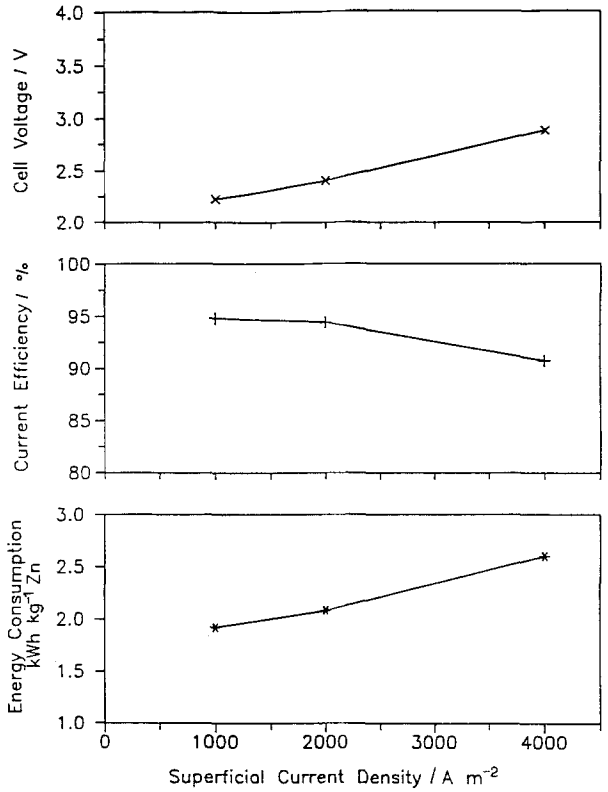

Fig. 8. Effect of superficial current density on the performance of fluidized bed cell. (Current feeder: lead; diaphragm: Celgard; anode: NE-A-30.)

cell voltage point of view. The cells with DSA and NE-A-30 gave lower cell voltages than the others. Due to the instability of DSA in strong alkaline solution, it cannot be used for a long run. The Pb/Celgard/NE-A-30 system consumed less than 2.1 kWh to electrodeposit a kilogram of zinc at a superficial current density of $2000\,A\,m^{-2}$.

The effect of superficial current density on the performance of the Pb/Celgard/NE-A-30 cell is shown in Fig. 8. In previous work on zinc deposition from acid electrolytes [19] hydrogen evolution was a problem at higher current densities and a maximum was observed in a plot of current efficiency against current density. However in the case of zinc electrodeposition from alkaline solution, as discussed previously, the standard electrode potential difference between zinc and hydrogen reduction reactions (0.42 V) is less than that of acid electrodeposition (0.76 V). Furthermore, the hydrogen overvoltage at a zinc electrode in potassium hydroxide solution is reported [9] to be approximately 0.9 V at an actual current density of $1000\,A\,m^{-2}$. While the hydrogen evolution current density (at the particle surface) would be much less in the present study, it appears that hydrogen evolution is kinetically disfavoured and electrodeposition of zinc proceeds at a high current efficiency which is relatively insensitive to current density.

4. Conclusion

Fluidized bed zinc electrodeposition from 45% potassium hydroxide zincate solution has been performed. The results indicate:

(i) that zinc particles can be regenerated without any operating problems by means of fluidized bed electrodeposition;
(ii) that lead and graphite are more suitable materials than copper in terms of current efficiency. When cell voltage is considered, lead appears superior to graphite;
(iii) that the NE-A-30 anode from Electrolyser Corporation has performed better than the other anodes tested;
(iv) that as a cell divider, Celgard from Hoechst Celanese Corporation has been stable throughout the electrolysis and yielded lower cell voltage than Daramic (W. R. Grace Co.).
(v) that the fluidized bed cell with a lead current feeder, Celgard diaphragm and NE-A-30 anode, showed a d.c. electrical energy consumption for zinc electrodeposition of $1.92\,kWh\,kg^{-1}$ of zinc at $1000\,A\,m^{-2}$ and $2.08\,kWh\,kg^{-1}$ at $2000\,A\,m^{-2}$ of superficial current density. Combining these numbers with figures from Part I, "round trip" energy efficiencies of 50% and 46%, respectively, are reached.

Acknowledgment

This work was supported by the Assistant Secretary for Conservation and Renewable Energy, Office of Energy Storage and Distribution, Energy Storage Division, of the U.S. Department of Energy under Contract No. DE-AC03-76SF00098.

References

[1] M. Dubrovsky, T. Huh, J. W. Evans and C. D. Carey, in 3rd International Symposium on Hydrometallurgy (edited by K. Osseo-Assare and J. D. Miller), TMS-AIME, Atlanta, GA (1983) 759.
[2] J. W. Evans and G. Savaskan, *J. Appl. Electrochem.* **21** (1991) 105–110.
[3] G. Savaskan, T. Huh and J. W. Evans, submitted to *J. Appl. Electrochem.* (1991).
[4] R. D. Amstrong and M. F. Bell, in Electrochemistry Vol. 4, A Special Periodic Report, The Chemical Society, Alden Press, London (1974) 1.
[5] J. P. Elder, *J. Electrochem. Soc.* **116** (1969) 757.
[6] N. A. Hampton, G. A. Herdman and R. Taylor, *Electroanal. Chem. & Interf. Electrochem.* **25** (1970) 9.
[7] J. O'M. Bocris, Z. Nagy and A. Damjanovic, *J. Electrochem. Soc.* **119** (1972) 285.
[8] A. R. Despic, Dj. Jovanovic and T. Rakic, *Electrochim. Acta* **21** (1976) 63.
[9] T. S. Lee, *J. Electrochem. Soc.* **122** (1975) 171.
[10] R. E. F. Einerhand, W. H. M. Visscher and E. Barendrecht, *J. Appl. Electrochem.* **18** (1988) 799.
[11] S. Arouete, K. F. Blurton and H. G. Oswin, *J. Electrochem. Soc.* **116** (1969) 166.
[12] R. D. Naybour, *ibid.* **116** (1969) 520.
[13] M. G. Chu, J. McBreen and G. Adzic, *ibid.* **128** (1981) 2281.
[14] E. Barendrecht, *ibid.* **129** (1982) 2654.
[15] T. Huh, Ph. D. Dissertation. U. C. Berkeley, Berkeley, CA (1985). [See also T. Huh and J. W. Evans, *J. Electrochem. Soc.* **134** (1987) 308–317 and **134** (1985) 317–321.]
[16] D. R. Gabe and D. C. Carbin, *Chem. Ind.* 19 April (1975) 335.
[17] A. J. Appleby, M. Chemla, H. Kita and G. Bronoel, 'Encyclopedia of electrochemistry of the elements', Vol. IX, Part A (edited by A. J. Bard), Marcel Dekker, New York (1984) p. 520.
[18] W. H. Dyson, L. A. Schreiner, W. P. Sholette and A. J. Salkind, *J. Electrochem. Soc.* **115** (1968) 566.
[19] V. Jiricny and J. W. Evans, *Met. Trans.* **15B** (1984) 623.